XRD ANALYSIS OF ILLITE-SMECTITE INTERSTRATIFICATION IN CLAYS FROM OIL SANDS ORES

B. Patarachao[1]*, D.D. Tyo[1], A. Zborowski[1], K. Davis, J. Kung[1], S. Ng[2], P.H.J. Mercier[1]

[1]National Research Council Canada (NRC), Ottawa, Ontario, Canada

[2]Syncrude Canada Ltd., Edmonton, Alberta, Canada

*bussaraporn.patarachao@nrc-cnrc.gc.ca

ABSTRACT

The presence of clays in oil sands, especially swelling clays such as smectite, has an adverse effect on bitumen recovery and tailings management. Identification and quantification of clay minerals are therefore important to the oil sands industry. Two estuarine (E3 and E7) and two marine (M13 and M18) oil sands were used in this study. Separation of <2 μm clay solids was accomplished using centrifugation technique based on Stokes' law. Comparison of XRD patterns produced from air-dried (AD) and ethylene-glycolated (EG) preparations confirmed the absence of discrete smectite, while revealing the presence of interstratified illite-smectite (I-Sm), illite and kaolinite as the primary clay minerals in these ores. Minor amounts of chlorite were found in significant quantities only in the marine ores. The degree of expandability owing to the presence of swelling (smectite) layers in the interstratified I-Sm component, measured using the intensity ratio (Ir) method available in the literature, showed that sample E7 has almost no tendency to swell while sample M13 has the highest degree of expandability. The plotting of Ir values vs. $FWHM_{(AD)}$ (Full width at half maximum of the illite 10Å peaks obtained from AD preparations) was used to estimate percentage of swelling layers. This indicated that the contents of swelling layers were 4–6% for M13 and M18, 2-4% for E3 and 0-2% for E7. By comparing two methods of measuring $FWHM_{(AD)}$ and Ir values, we conclude that these parameters may be quantified in a robust manner in XRD patterns from AD and EG preparations of <2um clays from oil sands ore. As the groupings of samples identified here in plotting $FWHM_{(AD)}$ vs. Ir values correlate well with batch-extraction unit bitumen recovery measured for the four ores, we suggest that this approach may represent a convenient way to assess the processability of oil sands ore.

INTRODUCTION

Clay mineralogy in oil sands has been studied extensively over the past few decades. Typically, clays amount to approximately 1–7 wt% of oil sand ores. Although clays are only present in small quantities, they are known to have adverse effects on bitumen recovery and tailings management. Identification and quantification of clay minerals are therefore important to the oil sands industry. Clay minerals from different oil sands sources and process streams such as ores, fine tailings and froth solids have been characterized (Ignasiak, *et al.*, 1983; Kotlyar, *et al*., 1985; Kotlyar *et al.*, 1987; Kotlyar *et al*., 1990; Ripmester *et al*., 1993; Omotoso *et al*., 2002; Omotoso

This document was presented at the Denver X-ray Conference (DXC) on Applications of X-ray Analysis.

Sponsored by the International Centre for Diffraction Data (ICDD).

This document is provided by ICDD in cooperation with the authors and presenters of the DXC for the express purpose of educating the scientific community.

Usage is restricted for the purposes of education and scientific research.

DXC Website
– www.dxcicdd.com

ICDD Website
- www.icdd.com

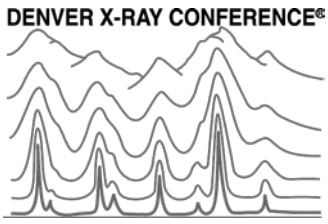

et al., 2006; Wallace *et al*., 2004; Kaminsky *et al*., 2009, Geramian *et al.,* 2016). Kaolinite, illite and chlorite were found to be the primary non-swelling clay minerals in oil sands. Smectite and interstratified clays such as kaolinite-smectite and illite-smectite were also reported as common swelling clays (Omotoso *et al*., 2006). In a previous study (Mercier *et al.,* 2008a) by our group, higher clay contents were found in marine ore compared to estuarine ore, leading to poor bitumen recovery in batch extraction unit tests. Specific surface area of illite on un-extracted ores, determined directly by powder X-ray Diffraction (XRD) analysis as per Mercier *et al.* (2008a,b), was also found to be significantly greater for four problematic ores. Up until now, various studies have been done on non-swelling clays in oil sands. However, little detail and information have been reported on the characteristics and properties of swelling clay minerals especially in oil sands ores. The presence of swelling clays such as interstratified illite-smectite (I-Sm) can be identified by comparing XRD patterns of air-dried (AD) and ethylene glycol-solvated (EG) oriented clay preparations (Moore and Reynolds, 1997). If significant amount of I-Sm is present, changes between patterns are observed. These changes include shifting in peak positions, emerging of new peaks, disappearance of certain peaks in the XRD patterns of EG preparation, etc. However, if only small content of I-Sm is present (<10% I-Sm), these criteria cannot be applied as the peak positions observed in the EG preparations very much resemble those of discrete illite. In this case, one of the key indicators for its presence is alteration of the shape of illite's first basal reflection (referred to here as the illite 10Å peak following nomenclature used in the literature), which becomes sharper and more symmetric as a result of ethylene glycol solvation treatment (Moore and Reynolds, 1997; Battaglia *et al*., 2004; Stern *et al*., 1995, Bozkaya *et al.*, 2016).A number of profile decomposition methods performed on the illite 10Å peak in XRD patterns of both AD and EG preparations explain the complexity of this multi-phase peak revealing the presence of I-Sm component in the highly illitic clays (Stern *et al*., 1991; Lanson and Besson, 1992; Wang *et al*., 1995). The degree of expandability owing to the presence of swelling (smectite) layers in the I-Sm component can be determined using the intensity ratio (Ir) of illite 10Å and illite 3.33Å diffraction peaks from the AD and EG preparation (Srodon, 1984 and 1980). Furthermore, the plotting of Ir values vs. $FWHM_{(AD)}$ (Full width at half maximum of the illite 10Å peaks obtained from AD preparations) can be used to estimate percentage of swelling layers (Velde and Eberl, 1989). This method has been widely accepted and used to study illitic components in sedimentary rocks but has never been applied to oil sands solids. In this study, we focus on confirming the presence of I-Sm clays in oil sand ores which were used in our previous study (Mercier *et al.*, 2008a) as well as determining the degree of expandability of this I-Sm component and estimating the percentage of swelling layers using the Ir and the plotting of Ir vs. $FWHM_{(AD)}$ as described above. The aim is to establish a relationship between degree of interstratification of I-Sm clays and processability of the oil sands. This approach may represent a convenient way to assess the processability of oil sands ore.

EXPERIMENTAL

Two estuarine ores (E3 and E7) and two marine ores (M13 and M18) were used in this study. Solids from oil sands ores were isolated by a toluene/water interfacial separation technique

(Mercier *et al*., 2019). With solids dispersed only in water, centrifugation with conditions based on Stokes' law was applied to yield <2um clay suspensions. Oriented clay slides were prepared for XRD analysis based on the Filter transfer method (Moore and Reynolds, 1997). Clay suspensions were Ca^{2+} saturated by adding ~50mg of $CaCl_2$ into 50mL of clay. 10mL of the Ca^{2+} saturated suspension was filtered onto a 0.45um type HE Millipore filter paper. The wet filter cakes were placed upside down on a glass slide and allowed to dry at room temperature for ~1 hr. The oriented clay slides were then subjected to the following treatments subsequently: *(1) Air drying (AD) at 54% relative humidity (RH)* - oriented clay slides were placed in a small desiccator containing super-saturated solution of magnesium nitrate in deionized water and were allowed to equilibrate for at least 24 hours. *(2) Ethylene glycol solvation (EG)* - oriented clay slides were placed in a small desiccator containing a Petri dish full of ethylene glycol, and the desiccator was placed in an oven at 65°C for 24 hours. *(3) Heat treatment at 375ºC for 2 hrs (HT375)* – oriented clay slides were placed in a muffle furnace and undergone heat treatment at 375ºC using heating rate of 10ºC/min under atmospheric condition. (4) *Heat treatment at 550ºC (HT550) for 2hrs* – oriented clay slides were placed in a muffle furnace and undergone heat treatment at 550ºC using heating rate of 10ºC/min under atmospheric condition. XRD measurements were performed after each treatment using powder X-ray diffractometer (XRD) - Bruker D8 Advance set up in Bragg Brentano geometry (theta-theta), configured with a Cobalt (Co) X-ray tube and a Position Sensitive Detector (VÅNTEC-1). XRD data were collected with a scan range of 4 to 30°2θ using a step size of 0.02 and a count time of 2 seconds per step. Peak fitting and decomposition of the illite 10Å and 3.33Å reflections was performed using Bruker TOPAS version 6 software through split-Pearson VII (SPVII) functions. Chebychev polynomial of 3rd order was used to model the background of the illite10Å peak covering the range 6-12°2θ. Rietveld refinement with standard crystallographic models (within the range 23-33°2θ with kaolinite 3.60Å peak region of 27-29.75°2θ excluded), was used to fit the diffraction peaks from quartz contaminant to overcome peak-overlapping issues between illite 3.33Å and quartz 3.36Å diffraction peak, allowing intensity of individual illite 3.33Å to be accurately determined. Degree of expandability was calculated using the intensity ratio (Ir) of the illite 10Å and illite 3.33Å diffraction peaks from the AD and EG preparations as shown in the equation below (Srodon, 1984).

$$\mathrm{Ir} = \frac{[I_{(10\text{Å})} / I_{(3.33\text{Å})}]_{\mathrm{AD}}}{[I_{(10\text{Å})} / I_{(3.33\text{Å})}]_{\mathrm{EG}}} \qquad (1)$$

In Equation 1, $I_{(10Å)}$ is the net intensity of illite 10Å diffraction peak and $I_{(3.33Å)}$ is the net intensity of illite 3.33Å diffraction peak. Percentage of swelling layers due to the presence of I-Sm was estimated using the plotting of Ir and $FWHM_{(AD)}$ (Eberl and Velde, 1989). The Ir and $FWHM_{(AD)}$ were determined using two different methods.

For Method 1: Ir was calculated using peak height intensity ratio of illite 10Å and illite 3.33Å peaks determined after background subtraction (Srodon, 1984). Two background positions were assigned on both sides of the diffraction peak. Background intensity were calculated using the following equation:

$$\text{Background intensity} = Bi_1 + \left[\left(\frac{Bi_2 - Bi_1}{Bp_2 - Bp_1}\right) \text{x } (Pp - Bp_1)\right] \qquad (2))$$

where Bi_1 is background intensity (counts) at the low 2θ angle side of the peak; Bi_2 is the background intensity (counts) at the high 2θ angle side of the peak; Bp_1 is the background position (º2θ) at the low 2θ angle side of the peak, Bp_2 is background position (º2θ) at the high 2θ angle side of the peak; and P*p* is the peak position (º2θ) at the observed maximum intensity of the peak. The value of $FWHM_{(AD)}$ of the illite 10Å peak was determined using one background on the high 2θ angle side of the peak as described by Eberl and Velde (1989).

For Method 2: Ir was calculated using integrated net area (counts º2θ) of the decomposed illite 10Å and illite 3.33Å peaks. Two SPVII diffraction lines were used to fit the illite 10Å peak whereas only a single SPVII line was used to fit the illite 3.33Å peak. The value of $FWHM_{(AD)}$ of the illite 10Å peak was determined as the integrated-area weighted sum of the two FWHM values (sum of h1 and h2 profile parameters) determined for each of the two individual SPVII lines refined with TOPAS to model the illite 10Å peak.

RESULTS

XRD patterns of different treatments for the <2 μm clay solids of samples E7, E3, M18 and M13 are shown in Fig. 1(a), 1(b), 1(c) and (1d), respectively. For the <2um clay solids of sample E7 separated from estuarine ore, illite and kaolinite are the main clay minerals present in this sample. No peaks were observed in the air-dried treatment at d-spacing above 15Å, indicating that there is no distinct smectite in detectable quantities. There is also no change in XRD patterns after ethylene glycol solvation nor after heat treatment at 375°C which further confirmed the absence of smectitic clay minerals. After heat treatment at 550ºC, the kaolinite structure was decomposed. If there is chlorite in this sample, a diffraction peak at 14.16Å would have appeared at this position. However, this reflection is not noticeable in this XRD pattern indicating that there is also no detectable chlorite in this sample. Similar observation was made for sample E3 separated from estuarine ore [Fig. 1(b)]. After all treatments, it was confirmed that illite and kaolinite are the main clay minerals, with no distinct smectite and no chlorite in detectable quantities. However, we noticed that in this sample the XRD pattern of the AD preparation showed a very broad and asymmetric shape with low-angle-side shoulder of illite 10Å reflection. This peak became sharper and more symmetric after EG treatment. This change is an indication of the presence of I-Sm clay mineral. For the <2um clay solids of M18 separated from marine ore, illite and kaolinite are still the main clay minerals. No distinct smectite is observed as there is no peak at a d-spacing value above 15Å in the AD treatment [Fig. 1(c)]. Alteration of illite 10Å peak shape between the AD and the EG preparations is more obvious in this sample. After heat treatment at 550ºC, the kaolinite structure was decomposed and this treatment also caused the intensity of the chlorite reflection at 14.16Å to increase which confirmed the presence of chlorite in this sample. It is noticed that higher order diffraction peaks related to untreated chlorite disappeared at this treatment temperature. The loss in their intensity is due to de-hydroxylation which is caused by the loss of the OH group as H_2O (Zhan and Guggenheim, 1995). A similar observation was made for the <2um clay solids of M13 sample compared to the

M18 sample [Fig.1(d)]. We also observed that the asymmetric illite 10Åpeak shape in the air-dried sample became sharper in the EG treatments. Chlorite is also present in this sample (M18) as we observed the increase in intensity of the chlorite reflection at 14.16Å after heat treatment at 550ºC.

Decomposition of illite 10Å diffraction peak in the AD pattern of sample E7 reveals the presence of a small component of I-Sm phase [Fig.2(a)]. This reflection appears at low-angle side of the peak. Upon EG treatment, a new I-Sm peak appears at higher-angle side of the peak. This peak corresponds to the I-$Sm_{(001/002)}$ reflection which appears as a broad band from 10.2-10.5 º2θ (8.66A-8.42Å). If the sample is rich in expandable I-Sm phases, the I-$Sm_{(001/001)}$ reflection can also be observed as a very low-intensity broad band with its maximum around 8.8 º2θ (11.6Å) (Battaglia, 2004; Lanson, 1991). In the case of sample E7, this reflection is very faint and hidden in the background. The effect of smectite interstratification became more pronounced in sample E3 [Fig.2(b)]. It is evident for E3 that sharpening of the illite 10Å diffraction peak upon ethylene glycol solvation was due to the appearance of low intensity I-Sm diffraction peaks towards lower (I-$Sm_{(001/001)}$) and higher (I-$Sm_{(001/002)}$) angle. The same effect is seen in sample M18 from marine ore as well as sample M13 as shown in Fig.2(c) and (d), respectively. It is also noticeable that not only the sharpening of the peak but the reduction in the intensity are observed after EG treatment, especially in sample M13. These changes are varied from one sample to another sample. It is noted that the I-$Sm_{(001/001)}$ reflection is hidden in the background and not visible in all samples. The degree of expandability owing to the presence of swelling (smectite) layer in the I-Sm component was measured using the intensity ratio *Ir* determined as shown in Equation 1.This ratio (Ir) is very sensitive to the presence of swelling layers in illite. If Ir>1.0, the illite has swelled to some degree; if Ir =1.0, the illite has no detectable tendency to swell (Srodon, 1984). Ir values determined from Method 1 and Method 2 are in good agreement as shown in Table 1. The Ir value of sample E7 is very close to 1 indicating very little to no swelling while sample M13 has the highest value of Ir showing the highest degree of expandability compared to the other samples. Values of $FWHM_{(AD)}$ obtained from the two methods are very close for sample E3 and E7, whereas more deviation is observed for sample M13 and M18 as the degree of expandability increases. Percentage of swelling layers (%) was estimated using the plotting of $FWHM_{(AD)}$ vs. Ir values established by Eberl and Velde (1989) as shown in Fig. 3. According to this plot, the contents of swelling layers were 4-6% for M13 and M18, 2-4% for E3 and 0-2% for E7. By comparing the two methods of measuring $FWHM_{(AD)}$ and Ir values used in this study, we determined the same contents of swelling layers for the four samples using either Method 1 or Method 2. We conclude that these parameters may be quantified in a robust manner in XRD patterns from AD and EG preparations of <2 μm clays from oil sands ore.

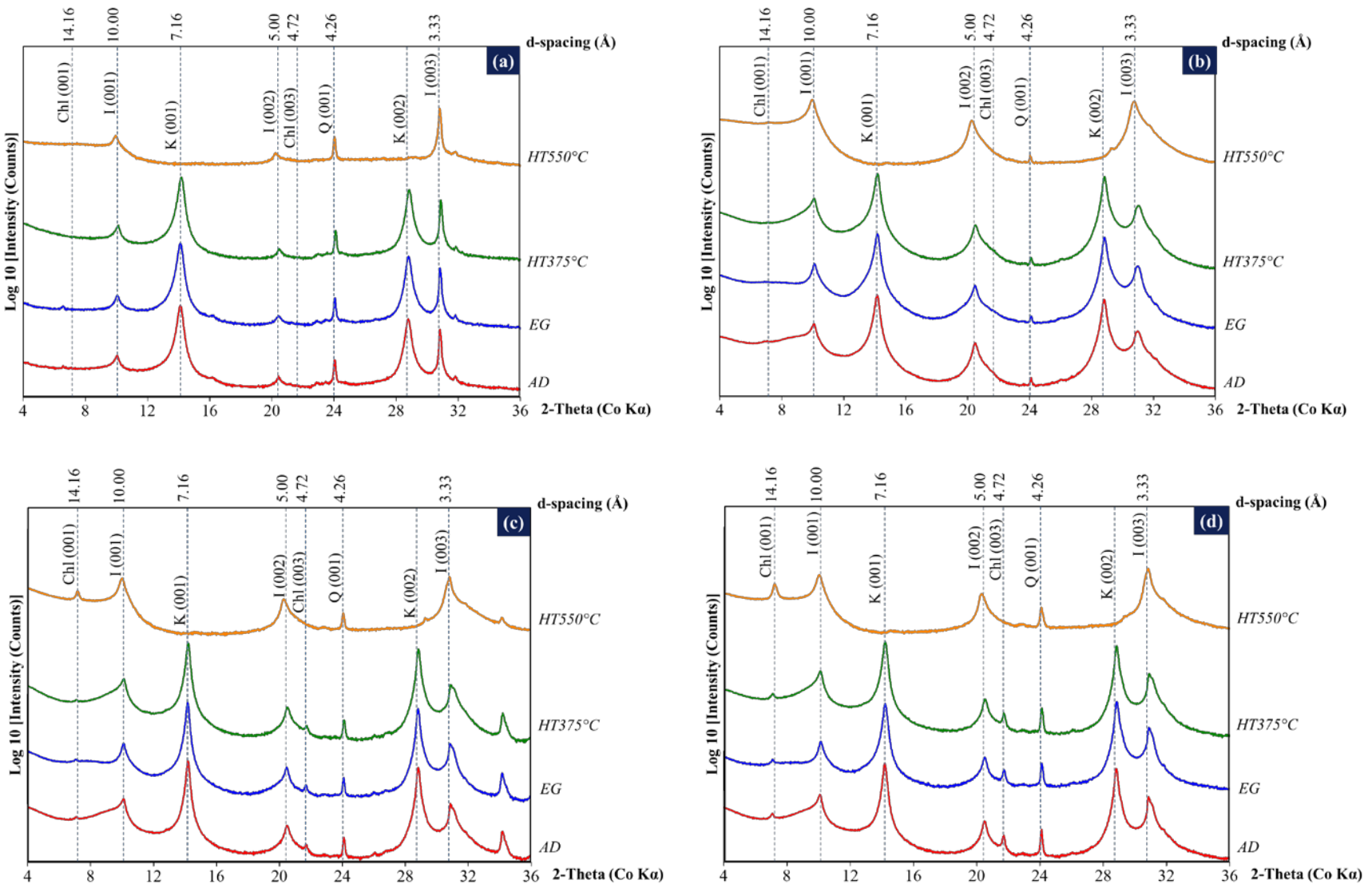

Fig. 1 XRD patterns of sample E7 (a), E3 (b), M18 (c) and M13 (d), K=Kaolinite, I=Illite, Chl=Chlorite, and Q=Quartz

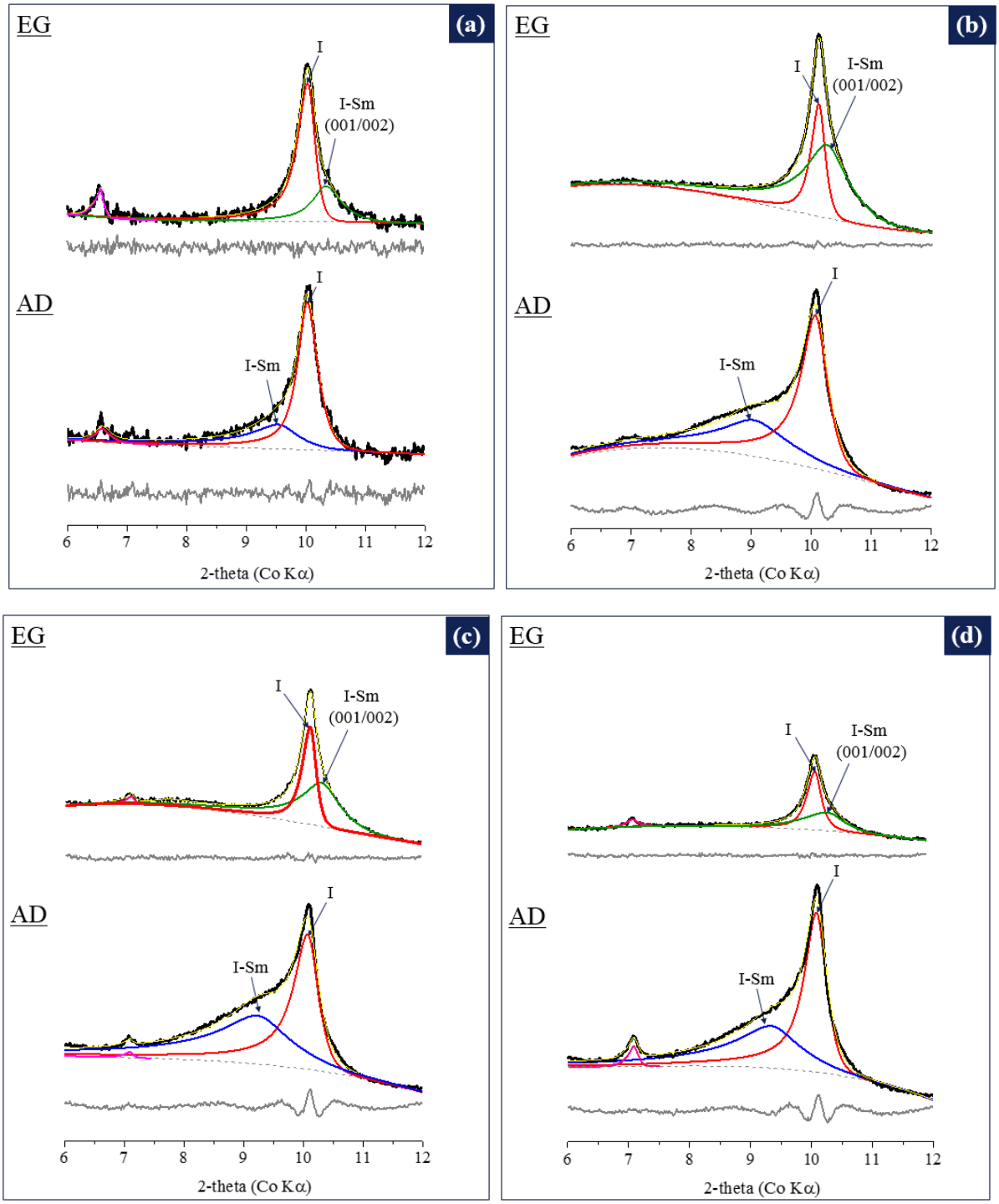

Fig. 2 Decomposition of the illite 10Å diffraction peak obtained from air-dried (AD) and ethylene glycolated (EG) preparations of sample E7 (a), E3 (b), M18 (c) and M13 (d).

It is shown in Table 1 that samples with content of swelling layer of 0-4% correlate to good bitumen recovery (E3 and E7) while samples with content of swelling layer of more than 4% correlate to poor bitumen recovery (M13 and M18). As the groupings of samples identified here in plotting $FWHM_{(AD)}$ vs. Ir values correlate well with batch-extraction unit (BEU) bitumen recovery measured for the four ores, we suggest that this approach may represent a convenient way to assess the processability of oil sands ore. This type of analysis has not previously been applied to oil sands ore and future work will be undertaken to evaluate the method further by its application to a much larger number of samples.

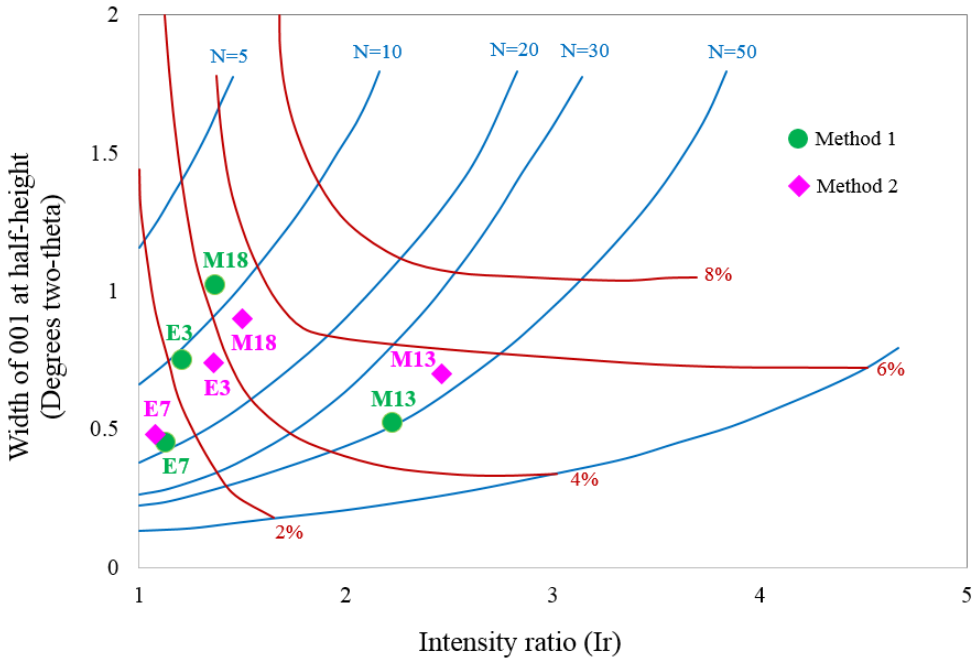

Fig. 3 $FWHM_{(AD)}$ vs Ir

Table 1 Intensity ratio (Ir), $FWHM_{(AD)}$, content of swelling layer and BEU results

Sample	Ir_1	Ir_2	$FWHM_{(AD)1}$	$FWHM_{(AD)2}$	Content of swelling layer	Total recovery (%bitumen)
E3	1.21	1.36	0.75	0.74	2-4%	93.3
E7	1.13	1.08	0.45	0.48	0-2%	92.4
M13	2.23	2.46	0.52	0.70	4-6%	31.7
M18	1.37	1.50	1.02	0.90	4-6%	57.5

[1]Values determined using method 1, [2] Values determined using method 2

CONCLUSIONS

Comparison of XRD patterns produced from air-dried (AD) and ethylene-glycolated (EG) preparations confirmed the absence of discrete smectite, while revealing the presence of

interstratified illite-smectite (I-Sm), illite and kaolinite as the primary clay minerals in these ores. Minor amounts of chlorite were found in significant quantities only in the marine ores. Higher degree of expandability of the interstratified I-Sm component was found in marine ores compared to estuarine ores with estimated percentages of swelling layers of 4-6% for M13 and M18, 2-4% for E3, and 0-2% for E7. Groupings of samples identified here in plotting FWHM vs. Ir values correlate well with batch-extraction unit bitumen recovery measured for the four ores. This approach may represent a convenient way to assess the processability of oil sands ore. Future work will be undertaken to evaluate the method further by its application to a much larger number of samples.

REFERENCES

Battaglia S., Leoni, L., Sartori F. (**2004)**. "The Kubler index in late diagenetic to low-grade metamorphic pelites; A critical comparison of data from 10A and 5A peaks," *Clays and Clay Minerals* **52**, 85-105.

Bozkaya, O., Gunal-Turkmenoglu, A., Goncuoglu, M.C., Unluce, O., Yilmaz, I.S., Schroeder, P.A. (**2016)**. "Illitization of Late Devonian-Early Carboniferous K-bentonites from Western Pontides, NW Turkey; Implications for their origin and age," *Applied Clay Science* **134**, 257-274.

Geramian, M., Osacky, M., Ivey, D.G., Liu, Q., Etsell, T.H. (**2016)**. "Effect of Swelling Clay Minerals (Montmorillonite and Illite-Smectite) on Nonaqueous Bitumen Extraction from Alberta Oil Sands," *Energy and Fuels* **30**, 8083-8090.

Ignasiak, T.M., Kotlyar, L., Longstaffe, F.J., Strausz, O.P., Montgomery D.S. (**1983)**. "Separation and Characterization of Clay from Athabasca Asphaltene," *Fuel* **62**, 353-362.

Kaminsky, H.W.A., Etsell, T.H., Ivey, D.G., Omotoso, O. (**2009)**. "Distribution of Clay Minerals in the Process Streams Produced by the Extraction of Bitumen from Athabasca Oil Sands," *The Canadian Journal of Chemical Engineer* **87**, 85-93.

Kotlyar, L.S., Kodama, H., Ripmester, R.A. (**1990)**. "Crystalline Inorganic Matter Present in Athabasca Oil Sands," *Appl. Clay Sci.* **5,** 1-12.

Kotlyar, L.S., Sparks, B.D., Grattan-Bellow, P.E. (**1987)**. "Non-Crystalline Inorganic Matter-Humic Complexes in Athabasca Oil Sand and their Relationship to Bitumen Recover," *Appl. Clay. Sci* **2**, 253-271.

Kotlyar, L.S., Sparks, B.D., Kodama, H. (**1985)**. "Isolation of Inorganic Matter-Humic Complexes from Athabasca Oil Sands," *Aostra. J. Res.* **2**, 103-111.

Lanson, B. and Besson, G. (**1992)**. "Characterization of the end of smectite-to-illite transformation: Decomposition of X-ray patterns," *Clays and Clay Minerals* **40**, 40-52

Mercier, P. H. J., Patarachao, B., Kung, J., Kingston, D.M., Woods, J.R., Sparks, B.D., Kotlyar, L.S., Ng, S., Moran, K. and McCracken, T. (**2008a)**. "X-ray diffraction (XRD)-derived

processability markers for oil sands based on clay mineralogy and crystallite thickness distributions," *Energy and Fuels* **22**, 3174-3193.

Mercier, P.H.J., Le Page, Y., Tu, Y. and Kotlyar, L. (**2008b)**. "Powder X-ray Diffraction Determination of Phyllosilicate Mass and Area versus Particle Thickness Distributions for Clays from the Athabasca Oil Sands," *Petroleum Science and Technology* **26**, 307-321.

Mercier, P.H.J., Tyo, D.D., Zborowski, A., Kung, J., Patarachao, B., Kingston, D.M., Couillard, M., Robertson, G., McCracken, T. and Ng, S. (**2019)**. "First Quantification of < 2 mm clay, < 0.2 mm Ultrafines and Solids Wettability in Process Streams from Naphthenic Froth Treatment Plant at Commercial Mined Oil Sands Operations," *Fuel* **237**, 961-976.

Moore D.M., Reynolds, R.C. (**1997**). *X-Ray Diffraction and the Identification and Analysis of Clay Minerals.* New York: Oxford University Press.

Omotoso, O., Mikula, R.J. and Stephens, P.W. (**2002**). "Interstratified Phyllosilicates in Athabasca Oil Sands from Synchrotron XRD," *Adv. X-ray Anal.* **45**, 391-396.

Omotoso, O., Mikula, R., Urquhart, S., Sulimma, H. and Stephens, P. (**2006**). "Characterization of Clays from Poorly processing Oil Sands Using Synchrotron Techniques," *Clay Sci.* **12**, 88-93.

Ripmeester, J.A., Kotlyar, L.S. and Sparks, B.D. (**1993**). "H NMR and the Sol-Gel Transition in Suspensions of Colloidal Clays," *Colloid Surf.* **78**, 57-63.

Srodon, J. (**1984**). "X-ray Powder Diffraction Identification of Illitic Materials," *Clays and Clay Minerals* **32**, 337-349.

Srodon, J. (**1980**). "Precise Identification of Illite/Smectite Interstratification by X-ray Powder Diffraction," *Clays and Clay Minerals* **28**, 401-411.

Stern W.B., Mullis, J., Rahn, M., and Frey, M. (**1991**). "Deconvolution of the First Illite Basal Reflection," *Schweizerische Mineralogische und Petrographische Mitteilungen* **71**, 453-462

Stern, W.B., Mullis, J., Rahn, M., Sun, M. and Frey, M. (**1995**). "On the shape of the first illite X-ray diffraction-reflection, crystallinity, and incipient metamorphism," *Revista Geologica de Chile* **22**, 127-135.

Velde, D.D., Eberl, B. (**1989**). "Beyond the Kubler index," *Clay Minerals* **24**, 571-577.

Wang, H., Stern, W.B. and Frey, M. (**1995**). "Deconvolution of the X-ray illite 10-Å complex: A case study of Helvetic sediments from eastern Switzerland," *Schweizerische Mineralogische und Petrographische Mitteilungen* **75**, 187-199.

Wallace, D., Tipman, R., Komishke, B., Wallwork, V. and Perkins, E. (**2004**). "Fines/Water Interactions and Consequences of the Presence of Degraded Illite on Oil Sands Extractability," *Can. J. Chem. Eng.* **82**, 667-677.

Zhan, W. and Guggenheim, S. (**1995**). "The Dehydroxylation of Chlorite and the Formation of Topotactic Product Phases," *Clays and Clays Minerals* **43**, 622-629.